

# Effects of Hyperthyroidism on Adipose Tissue Activity and Distribution in Adults

Karen Geva Steinhoff,<sup>1,\*</sup> Kerstin Krause,<sup>2,\*</sup> Nicolas Linder,<sup>3,4</sup> Michael Rullmann,<sup>1,4</sup> Lisa Volke,<sup>2</sup> Claudia Gebhardt,<sup>2,5</sup> Harald Busse,<sup>3</sup> Michael Stumvoll,<sup>2,4,5</sup> Matthias Blüher,<sup>2,4,5</sup> Osama Sabri,<sup>1</sup> Swen Hesse,<sup>1,4,†</sup> and Anke Tönjes<sup>2,†</sup>

**Background:** Positron emission tomography (PET) has provided evidence that adult humans retain metabolically active brown adipose tissue (BAT) depots. Thyroid hormones (TH) stimulate BAT thermogenesis by central and peripheral mechanisms. However, the effect of hyperthyroidism on BAT activity and BAT volume in humans is yet not fully understood. The aim of this study was to investigate the effect of TH on (i) the metabolic activity of brown and white adipose tissue (WAT) depots, (ii) on abdominal visceral and subcutaneous adipose tissue area, and (iii) on serum levels of metabolically active cytokines.

**Methods:** Nineteen patients with overt hyperthyroidism were investigated through repeated 2-[<sup>18</sup>F]fluoro-2-deoxy-D-glucose positron emission tomography/computed tomography (2-[<sup>18</sup>F]FDG PET/CT) in the hyperthyroid and in the euthyroid state. The 2-[<sup>18</sup>F]FDG uptake was calculated as standard uptake ratio with blood pool as reference. Fat areas were quantified by means of CT segmentation. Serum levels of fetuin A and B, fibroblast growth factor 21, adipocyte fatty acid-binding protein (AFABP), retinol-binding protein 4, proenkephalin, pro-neurotensin, and neuregulin 4 were determined in the hyperthyroid and in the euthyroid state for each subject.

**Results:** 2-[<sup>18</sup>F]FDG uptake was increased in the hyperthyroid state in BAT in comparison with the euthyroid phase ( $p=0.001$ ). There was no correlation between serum free triiodothyronine (fT3) and free thyroxine (fT4) levels and 2-[<sup>18</sup>F]FDG uptake in BAT or WAT. In the hyperthyroid state, fT3 levels were positively associated with skeletal muscle standardized uptake value ratios. Areas of visceral adipose tissue and skeletal muscle were significantly decreased in hyperthyroidism. AFABP levels correlated positively with fT3 ( $p=0.031$ ,  $\beta=0.28$ ) and fT4 ( $p=0.037$ ,  $\beta=0.27$ ) in the hyperthyroid state.

**Conclusions:** Our results suggest that the contribution of increased TH levels to the glucose uptake of BAT and WAT is low compared with that of the skeletal muscle. Hyperthyroid subjects have reduced areas of visceral adipose tissue and increased AFABP levels.

**Keywords:** brown adipose tissue, thyroid dysfunction, hyperthyroidism, adipokines, white adipose tissue, positron emission tomography, computed tomography, fluorodesoxyglucose

## Introduction

**T**HYROID HORMONE (TH) is an important regulator of energy homeostasis. TH maintains basal metabolic rate, facultative and adaptive thermogenesis; modulates appetite and food intake; and regulates body weight (1). Under normal physiological conditions, the hypothalamic–pituitary–thyroid axis maintains stable TH levels, resulting in a

constant contribution of TH on to energy expenditure and energy homeostasis. Changes in the thyroidal state are frequently associated with alterations of the metabolic rate due to effects in key metabolic pathways that control energy expenditure and energy storage in particular through actions in the brain, skeletal muscle, liver, and brown adipose tissue (BAT) (2,3). BAT is a direct target of TH and can be activated via central and peripheral action (4). Further, several studies

<sup>1</sup>Department of Nuclear Medicine; <sup>2</sup>Medical Department III–Endocrinology, Nephrology, Rheumatology; <sup>3</sup>Department of Radiology; University of Leipzig Medical Center, Leipzig, Germany.

<sup>4</sup>Integrated Research and Treatment Center (IFB) Adiposity Diseases Leipzig, Leipzig, Germany.

<sup>5</sup>Helmholtz Zentrum München, Helmholtz Institute for Metabolic, Obesity and Vascular Research, Leipzig, Germany.

\*These authors have contributed equally to this work as first authors.

†These authors have contributed equally to this work as corresponding authors.

suggest that TH also induces the recruitment of “beige” adipocytes in white adipose depots, a process known as browning. The BAT utilizes fatty acids and glucose to regulate body temperature through activation of uncoupling protein 1, which uncouples the mitochondrial electron transport to produce heat instead of ATP (5). Mainly because of its ability to use glucose and lipids for thermogenesis, BAT has been regarded as a promising target for combating obesity and its related metabolic disorders in humans (6). However, similar to white adipose tissue (WAT), BAT has a secretory role, which could support the systemic effects of BAT activity. Among many compounds, fibroblast growth factor 21 (FGF-21) and neuregulin 4 (Nrg4) are important “Batokines” that promote glucose disposal and attenuate hepatic lipogenesis, respectively (7). Further, Nrg4 and FGF-21 have thermogenic properties by enhancing sympathetic innervation of BAT and WAT and induction of PGC1 $\alpha$ , respectively (8,9). There is evidence that TH interacts with cytokines secreted from BAT, WAT, or liver, which not only may have thermogenic properties but also may contribute to the regulation of whole-body metabolism. For instance, it has been shown that leptin, adiponectin, retinol-binding protein 4 (RBP4), adipocyte fatty acid-binding protein (AFABP), and fetuin A and B are influenced by the TH level (10–14). For other compounds, such as pro-enkephalin (pro-ENK) and pro-neurotensin (pro-NT), it is not yet known whether the secretion profile is influenced by TH.

The BAT is present and metabolically active in human adults and can be detected in adults with fluorine-18 labeled fluoro-2-deoxy-D-glucose (2-[<sup>18</sup>F]FDG) and positron emission tomography/computed tomography (PET/CT) imaging (15). However, whether and to what extent TH induces brown and beige fat activity in humans is not fully understood and study results are contradictory. A recent retrospective analysis of a large number of 2-[<sup>18</sup>F]FDG PET/CT scans of patients without thyroid disease revealed higher thyrotropin (TSH) values and lower visceral adipose tissue mass in the BAT positive, predominantly euthyroid group (16). Further, active BAT has been found in individuals with higher TSH levels after thyroidectomy but without significant differences in BAT activation related to TH levels (17), while others found 2-[<sup>18</sup>F]FDG uptake in BAT only in euthyroid individuals but not in study participants with hyper- or hypothyroidism (18). Overall, the predominance of active BAT in patients cohorts with altered thyroid function appears to be not different from those seen with 2-[<sup>18</sup>F]FDG PET/CT BAT studies in individuals without altered thyroid function based on retrospective analyses (16,19,20). Finally, one retrospective study reported an inverse correlation between the probability of detecting BAT and high thyroidal glucose uptake (21). In several studies investigating the impact of thyroid function on BAT activation, study participants were exposed to cold temperatures to further trigger BAT activation as it is common practice in nonthyroid-related BAT activation studies (22–26). Altogether, these studies demonstrated inconsistent results most likely due to heterogeneity in subject characteristics and differences in the study design (27). Thus, prospective investigations on the relationship between thyroid states and BAT activity are necessary without amplifying BAT activation by cold stress.

Therefore, we investigated the direct effects of TH on activation of adipose tissue and skeletal muscle in a pro-

spective cohort study of subjects in the hyper- and the euthyroid state by 2-[<sup>18</sup>F]FDG-PET/CT imaging at ambient room temperature. Further, we aimed at elucidating the association between levels of TH, adipokines, hepatokines, and changes in areas of white fat depots as well as skeletal muscle.

## Materials and Methods

### Study protocol

The study was conducted in accordance with the principles of the Declaration of Helsinki. Thirty individuals (19 females; mean age: 50.4 years ranging from 21 to 67 years) with hyperthyroidism (mean free triiodothyronine [fT3]: 12.8 pmol/L, range 6.4–47.9 pmol/L, mean free thyroxine [fT4] 28.8 pmol/L, range 10.8–90.2 pmol/L) were recruited at the University Hospital of Leipzig between November 2013 and August 2016. All individuals provided written informed consent before study participation. During baseline examination, all individuals were in the hyperthyroid state and 22 of them underwent the follow-up examination after reaching the euthyroid state. Sixteen individuals received radioiodine therapy, of whom 10 did not receive any thyroid specific medication and 7 subjects were on levothyroxine therapy at the follow-up examination. Three study participants had not received definite intervention at the time point of the second PET/CT, including two individuals who were euthyroid under therapy with methimazole and one individual who was euthyroid without specific medication.

At both time points, body mass index (BMI), waist-to-hip ratio, axillary body temperature, heart rate (HR), nicotine use, and physical activity were determined. Further, at both study visits, a 2-[<sup>18</sup>F]FDG PET/CT and blood samples, after overnight fasting, were performed. All tests were performed at ambient room temperature (20°C–22°C). Two study participants were excluded from the follow-up due to recurrence of hyperthyroidism and 1 study participant due to unexpected mild hypothyroidism, resulting in 19 study participants who remained in follow-up for analysis. The study was approved by regulatory authorities (*Bundesamt für Strahlenschutz*; No: Z5–22463/2–2013-010) as well as by the local ethics committee (Reg. No: 410-12-17122012).

### Serum analysis

In all study participants, blood samples were taken in the morning after an overnight fast and were immediately spun and frozen at –80°C until analyses were performed. Serum concentrations of AFABP, fetuin A, fetuin B, FGF-21 RBP4, and Nrg4 were determined with commercially available enzyme-linked immunosorbent assays according to the manufacturer’s instructions (AFABP, fetuin A, fetuin B and FGF-21: BioVendor, Inc., Brno, Czech Republic; RBP4: Adipogen, Inc., San Diego; Nrg4: Phoenix Pharmaceuticals, Inc., Burlingame). Serum concentrations of pro-NT and pro-Enk were quantified by sphingotec (Sphingotec GmbH, Hennigsdorf, Germany) by using a previously validated chemiluminometric sandwich immunoassay (28). Fasting insulin, fasting glucose, fT3, fT4, and TSH were measured by standard laboratory methods in a certified laboratory (University of Leipzig, Institute of Laboratory Medicine, Clinical Chemistry and Molecular Diagnostics).

### PET/CT imaging

The study participants were examined after 12 hours of fasting period with plasma glucose in the normal range. They were instructed to drink at least 1 L of water during the fasting period to ensure a sufficient hydration status. Adapted to body weight, an average activity of 296 MBq 2-[<sup>18</sup>F]FDG (range 203–384 MBq) was administered intravenously for each PET scan. To reduce the participant's radiation dose and enhance image quality by reducing background activity, 40 mg furosemide was given intravenously 5 minutes after tracer injection. Study participants wore regular clothing, and room temperature was kept between 20°C and 22°C for at least 30 minutes before tracer injection to the end of the PET/CT scan. Blood sampling was performed immediately before injection of the tracer.

The 2-[<sup>18</sup>F]FDG PET/CT images from skull base to umbilicus were obtained after a 60–90 minutes uptake period by using a standard imaging protocol on a PET/CT scanner (Biograph16; Siemens Healthcare, Erlangen, Germany) with 4 minutes per bed position for PET acquisition, standardized data reconstruction, and postprocessing in accordance with European guidelines (29). Low-dose CT imaging was performed (120 kV, 25 mAs).

### PET data analysis

Semiquantitative volume of interest (VOI) analyses was performed in each PET scan by using CT-based VOIs manually defined for supraclavicular BAT, visceral WAT (vWAT), deep subcutaneous WAT (dWAT), superficial subcutaneous WAT (sWAT), liver, and mediastinal blood pool using a software (Hermes Hybrid Viewer; Hermes Medical Solutions AB, Sweden). In each transaxial slice, the VOI was checked and adjusted manually to exclude nonfatty tissue such as vessels or small muscles in the BAT and WAT VOI as well as blood vessel wall or muscle activity in the blood pool VOI. Further, skeletal muscle VOI was defined individually in parts of shoulder and/or neck muscles without visually detectable focal increased muscle 2-[<sup>18</sup>F]FDG uptake. In each VOI, 2-[<sup>18</sup>F]FDG uptake was measured by using mean standardized uptake value (SUV<sub>mean</sub>), and tissue density was measured by using mean Hounsfield Units. In accordance with previous published protocols, mean liver as well as blood pool SUV<sub>mean</sub> was used as a reference for semiquantitative BAT and WAT analysis (27,30,31). In particular, SUV ratios (SUVR) for BAT, vWAT, dWAT, sWAT, and skeletal muscle 2-[<sup>18</sup>F]FDG uptake were determined by calculation of the ratio of the respective SUV<sub>mean</sub> to liver and blood pool SUV<sub>mean</sub>. For statistical analysis, only SUVR normalized to blood pool SUV<sub>mean</sub> were used.

### CT-based analysis of adipose tissue areas

CT images were segmented by using a custom-made software tool running under IDL (Exelis, Boulder, CO), as previously published (32). Tissue-specific thresholds for adipose (−190 to −30 HU) and muscle (−29 to 150 HU) tissue were selected, a click-wise selection of the regions of interest was performed, and results were controlled by a histogram (Supplementary Fig. S1). The resulting areas represent total adipose tissue (A<sub>TAT</sub>), visceral adipose tissue (A<sub>VAT</sub>), subcutaneous adipose (A<sub>SAT</sub>), total muscle (A<sub>MTOT</sub>), Psoas

muscle (A<sub>MPSO</sub>), paraspinous muscle (A<sub>MSPI</sub>), and ventral abdominal wall muscle (A<sub>MVEN</sub>). The skeletal muscle index was calculated as reported by Martin *et al.* (33). Mean muscle attenuation was determined (31), with the exception of A<sub>MVEN</sub>, which was excluded because of its small volume, making it prone to partial volume effects.

### Statistical analysis

For statistical analysis, SPSS software version 24.0 (IBM, Armonk, NY) was used. Differences between hyperthyroid and euthyroid state were assessed by Wilcoxon rank test for paired samples. Individual ratios between the hyperthyroid and the euthyroid state were calculated for each parameter of interest. Correlation analysis between adipokines, fat areas, SUV<sub>R</sub> as a surrogate marker of glucose metabolism, and thyroid markers was performed by using the rank correlation method indicated by Kendall-Tau. To identify independent associations of adipokines with thyroid state and body fat, a multiple linear regression analysis was performed. Before multiple linear regression, all variables were logarithmically transformed. Normal distribution of residuals was checked by the Shapiro–Wilks test. A *p*-value of <0.05 was considered statistically significant in all analyses. Correction for multiple testing was performed by Bonferroni correction test.

## Results

### Subject characteristics

Baseline characteristics of the study population are shown in Table 1. All study participants showed suppressed TSH levels and elevated TH levels at the time of the first PET/CT scan. At the time of the second PET/CT scan, TSH and TH levels were within the normal range. Mean age of the study cohort in the hyperthyroid state was 46.3 ± 13.6 and 50.4 ± 13 years at euthyroid follow-up examination. The average follow-up time was 186 days (range 101–577 days, median 186 days, mean 243 days). There were no significant differences in either sex, body temperature, physical activity, or nicotine use of subjects between the hyperthyroid and euthyroid state nor of outdoor temperature at the time point of the PET/CT scan imaging. However, there were significant differences in BMI, HR, fasting blood glucose, fasting insulin, fT3, fT4, and TSH (Table 1).

### Association between TH and 2-[<sup>18</sup>F]FDG uptake in WAT and BAT depots

Hyperthyroidism was associated with visually altered 2-[<sup>18</sup>F]FDG biodistribution with high activity in the entire skeletal muscle, while 2-[<sup>18</sup>F]FDG uptake in BAT regions visually did not differ from that of the surrounding tissue. The SUV analysis revealed a significantly decreased liver uptake (SUV<sub>mean</sub>: 2.18 ± 0.37 vs. 2.45 ± 0.29, median 2.24 vs. 2.42, *p* = 0.001) together with a significant reduction of blood pool uptake (SUV<sub>mean</sub>: 1.38 ± 0.29 vs. 1.57 ± 0.23, median 1.37 vs. 1.61, *p* = 0.014) in hyperthyroid state compared with the euthyroid state in the paired analysis. Further, SUV<sub>mean</sub> in skeletal muscle was significantly increased by 28.8% in hypothyroidism versus euthyroidism (SUV<sub>mean</sub>: 0.98 ± 0.25 vs. 0.70 ± 0.10, median 0.96 vs. 0.69, respectively, *p* < 0.001).

To eliminate the influence of general 2-[<sup>18</sup>F]FDG biodistribution changes to the measured TH-dependent adipose

TABLE 1. BASELINE CHARACTERISTICS OF STUDY COHORT

	N	Hyperthyroid	N	Hyperthyroid	Euthyroid	Median $\Delta$	p	Power
BMI, kg/m <sup>2</sup>	30	24.8 (22.5 to 28.8)	19	24.8 (23.1 to 28.7)	26.6 (23.4 to 29.6)	-1 (-1.9 to -0.2)	<b>0.001</b>	0.97
WHR	30	0.92 (0.84 to 0.96)	18	0.93 (0.88 to 0.99)	0.93 (0.88 to 0.97)	0 (-0.03 to 0.03)	0.966	0.07
HR	30	76 (68 to 80)	19	76 (68 to 80)	60 (60 to 72)	12 (4 to 20)	<b>0.002</b>	0.93
ft3, pmol/L	30	9.57 (8.18 to 16)	18	9.79 (8.17 to 14.22)	4.65 (4.14 to 4.97)	5.09 (3.56 to 9.86)	<b>&lt;0.001</b>	1
ft4, pmol/L	30	25.95 (20.64 to 29.9)	18	26.58 (21.97 to 29.9)	15.6 (12.86 to 17.46)	11.19 (4.39 to 15.4)	<b>&lt;0.001</b>	1
FG, pmol/L	30	5.43 (4.84 to 5.79)	18	5.49 (5.07 to 5.93)	5.33 (4.93 to 5.63)	0.2 (0.05 to 0.69)	<b>0.029</b>	0.55
FI, pmol/L	30	61.65 (37.58 to 102.88)	18	56.55 (37.58 to 112.15)	50 (34.03 to 79.45)	10.55 (-4.78 to 20.38)	<b>0.023</b>	0.63
TSH, mU/L	30	0.003 (0.003 to 0.003)	18	0.003 (0.003 to 0.004)	1.07 (0.779 to 1.505)	-1.06 (-1.5 to -0.78)	<b>&lt;0.001</b>	1
Fetuin A, $\mu$ g/mL	19	319 (292 to 343)	15	308 (291 to 343)	273 (249 to 321)	35 (15 to 60)	<b>0.018</b>	0.69
Fetuin B, ng/mL	19	3035 (2535 to 3917)	15	3035 (2673 to 3513)	2680 (2354 to 2797)	424 (159 to 764)	<b>0.001</b>	0.91
FGF-21, pg/mL	30	122.2 (52.8 to 155)	18	86.4 (37.9 to 155)	111.3 (13.4 to 205.3)	4.5 (-0.8 to 9.3)	0.669	0.1
AFABP4, ng/mL	30	21.6 (18.6 to 31.2)	18	21.5 (16.7 to 29)	18.5 (14.3 to 28.8)	-4.6 (-100.4 to 53.7)	<b>0.016</b>	.56
RBP4, $\mu$ g/mL	30	30.4 (23.7 to 37.1)	18	27.7 (23.7 to 37)	36.3 (31 to 42.5)	-9.7 (-16.2 to 2)	<b>0.048</b>	0.52
pro-ENK, pmol/L	30	56.7 (48.5 to 62.8)	18	52 (44.4 to 59.9)	51 (43.8 to 59.8)	0.4 (-8.8 to 11.5)	0.766	0.06
pro-NT, pmol/L	30	85.5 (63.6 to 112.1)	18	78.2 (58.6 to 112)	96.8 (78.2 to 116.3)	-4.5 (-29.1 to 1.7)	0.054	0.49
Nrg4, ng/mL	21	11.1 (9.3 to 13)	18	10.6 (8.6 to 12.1)	10.9 (9.0 to 11.8)	0.5 (-0.6 to 1.9)	0.347	0.38

Values are provided as median (interquartile range). Statistical test was applied to paired samples only, using Wilcoxon rank test for paired samples. Exact two-tailed *p*-values are depicted. Significant *p*-values ( $\alpha < 0.05$ ) are highlighted in bold.

AFABP4, adipocyte fatty acid-binding protein 4; BMI, body mass index; FG, fasting glucose; FGF, fibroblast growth factor; FI, fasting insulin; FT3, free triiodothyronine; FT4, free thyroxine; HR, heart rate; Nrg4, neuregulin 4; pro-ENK, pro-enkephalin; pro-NT, pro-neurotensin; RBP4, retinol-binding protein 4; TSH, thyrotropin; WHR, waist-to-hip ratio.

tissue  $SUV_{mean}$ , we performed a further semiquantitative analysis by using blood pool and liver  $SUV_{mean}$  as reference. Both SUVR did not reveal significantly different results. However, the hepatic glucose metabolism is known to be TH dependent (34) and might mask TH-induced changes in [<sup>18</sup>F]FDG uptake in other tissues. To avoid this bias, we used the SUVR normalized to blood pool activity for further semiquantitative analyses. Thus, by normalizing the 2-[<sup>18</sup>F]FDG uptake to blood pool  $SUV_{mean}$ , we detected a significant increase in SUVR in the hyperthyroid state in BAT and vWAT (Table 2). Compared with the euthyroid control, SUVR was 36% higher in BAT and 18% higher in vWAT in the hyperthyroid state as compared with the euthyroid stage. No significant differences were detected for dWAT and sWAT SUVR. The SUVR for skeletal muscle was 38% higher in hyperthyroid state compared with euthyroid state (Table 2).

#### Univariate correlations between TH levels and SUVR in adipose tissue and skeletal muscle

Despite the differences in group analysis for hyperthyroid and euthyroid state, in univariate correlation analyses TH levels did not correlate significantly with the respective SUVR of BAT and WAT depots, neither in the hyperthyroid nor in the euthyroid state (Fig. 1). However, TSH level correlated significantly with the SUVR in sWAT in the euthyroid state ( $\tau_b = 0.346$ ,  $p = 0.045$ ; Supplementary Table S2). Consistent with the group analysis, ft3 levels correlate significantly in univariate correlation analyses with skeletal muscle SUVR in hyperthyroid ( $\tau_b = 0.430$ ,  $p < 0.001$ ) but not in the euthyroid state (Supplementary Tables S1 and S2, respectively).

#### Association between TH levels and distribution of adipose depots and skeletal muscle

Fat and muscle segmentation revealed a significant decrease in  $A_{TAT}$ , in hyperthyroid as compared with the euthyroid state (Table 2). In particular,  $A_{VAT}$  was significantly decreased in the hyperthyroid as compared with the euthyroid state ( $p = 0.006$ ) while  $A_{SAT}$  did not differ (Table 2). Likewise,  $A_{MTOT}$  was significantly lower in the hyperthyroid versus the euthyroid state ( $p = 0.009$ ). In the hyperthyroid state, BAT SUVR was negatively associated with  $A_{TAT}$  and  $A_{VAT}$  ( $p = 0.032$  and  $p = 0.004$ , respectively, Supplementary Table S1).

To analyze whether the change in the  $A_{TAT}$  and skeletal muscle is related to TH levels, we performed Kendall-Tau correlation analysis. As shown in Supplementary Table S1, in the hyperthyroid state we detected no correlation of adipose tissue and skeletal muscle areas with ft3. However, ft4 were negatively associated with  $A_{MTOT}$  ( $p = 0.049$ ) but not with the areas of different adipose depots (Supplementary Table S1).

We next calculated ratios between TH levels in the hyperthyroid and euthyroid state (HY/EU) to determine changes in  $A_{TAT}$  and  $A_{MTOT}$  on changing serum TH levels. Kendall-Tau correlation analysis revealed a negative association between ft3 ratios (HY/EU) and  $A_{TAT}$  ( $\tau_b = -0.373$ ;  $p = 0.031$ ) as well as with  $A_{VAT}$  ( $\tau_b = -0.373$ ;  $p = 0.031$ ; Supplementary Table S3). Neither ratios of ft3 nor ft4 correlated significantly with areas of  $A_{MTOT}$  (Supplementary Table S3).

TABLE 2. 2-[<sup>18</sup>F]FDG UPTAKE IN WHITE AND BROWN ADIPOSE TISSUE DEPOSITS, SKELETAL MUSCLE (STANDARDIZED UPTAKE VALUE RATIO), AND AREAS OF FAT AND SKELETAL MUSCLE

	N	Hyperthyroid	N	Hypothyroid	Euthyroid	Median $\Delta$	p	Power
<b>Glucose uptake, SUVR</b>								
BAT	30	0.36 (0.26 to 0.45)	19	0.35 (0.26 to 0.39)	0.23 (0.2 to 0.3)	0.09 (0.02 to 0.14)	<b>0.001</b>	0.95
dWAT	30	0.14 (0.13 to 0.18)	19	0.14 (0.13 to 0.18)	0.14 (0.12 to 0.16)	0.01 (-0.01 to 0.04)	0.241	0.15
sWAT	30	0.11 (0.09 to 0.14)	19	0.12 (0.09 to 0.14)	0.11 (0.1 to 0.14)	0 (-0.03 to 0.02)	0.860	0.06
vWAT	30	0.28 (0.21 to 0.34)	19	0.28 (0.19 to 0.34)	0.23 (0.17 to 0.27)	0.04 (-0.02 to 0.07)	0.087	0.39
SM	30	0.68 (0.56 to 0.85)	19	0.63 (0.55 to 0.76)	0.42 (0.38 to 0.5)	0.2 (0.08 to 0.29)	< <b>0.001</b>	1
<b>Fat and muscle area, mm<sup>2</sup></b>								
A <sub>TAT</sub>	29	344.8 (247.8 to 394.95)	19	344.8 (248.2 to 392.9)	391.3 (274.5 to 436.7)	-39.1 (-80.8 to -3.1)	<b>0.004</b>	0.88
A <sub>VAT</sub>	29	82 (58.4 to 142.3)	19	103.7 (62.2 to 166.3)	127.7 (69.8 to 171.2)	-21.2 (-42.4 to 1.5)	<b>0.006</b>	0.8
A <sub>SAT</sub>	29	190.1 (157.95 to 254.95)	19	173.3 (159.6 to 248.9)	210.5 (154.1 to 274.4)	-10.6 (-26.3 to 5.5)	0.096	0.45
A <sub>MTOT</sub>	29	112.6 (101.05 to 147.3)	19	118.2 (102.5 to 157.8)	116.1 (111.3 to 184.4)	-9.7 (-21.2 to 1.6)	<b>0.009</b>	0.8
A <sub>MPSO</sub>	29	16.7 (13.35 to 22)	19	18.3 (13.5 to 23.1)	17.7 (15.4 to 21.7)	-5.8 (-8.6 to -0.7)	0.358	0.12
A <sub>MVEN</sub>	29	48.4 (42.3 to 72.3)	19	57.8 (43.1 to 77.3)	51.4 (47.5 to 86.4)	-2.9 (-10 to 1.3)	0.123	0.39
A <sub>MSPI</sub>	29	48.4 (43.05 to 58.45)	19	51.4 (43.5 to 59)	52.9 (46.5 to 66.5)	-1 (-3.1 to 1.4)	<b>0.001</b>	0.98
MA	29	38.21 (29.98 to 41.42)	19	38.2 (28.6 to 41.5)	38.43 (34.34 to 40.83)	-0.13 (-3.62 to 2.03)	0.490	0.13
SMI	29	40.38 (36.08 to 45.12)	19	41.88 (37.4 to 48.8)	42.79 (40.5 to 53.5)	-2.96 (-6.04 to 0.6)	<b>0.012</b>	0.78

Glucose uptake in WAT and BAT deposits (SUVR), fat, and muscle area in study cohort.

Statistical test was applied to paired samples only, using Wilcoxon rank test for paired samples. Values are provided as median (interquartile range). Exact two-tailed *p*-values are depicted. Significant *p*-values ( $\alpha < 0.05$ ) are highlighted in bold.

A<sub>MPSO</sub>, Psoas muscle area; A<sub>MSPI</sub>, paraspinal muscle area; A<sub>MVEN</sub>, ventral abdominal wall muscle area; A<sub>SAT</sub>, subcutaneous adipose tissue area; A<sub>TAT</sub>, total adipose tissue area; A<sub>VAT</sub>, visceral adipose tissue area; BAT, brown adipose tissue; dWAT, deep white adipose tissue; MA, mean muscle attenuation; SM, skeletal muscle; SMI, skeletal muscle index; SUVR, standardized uptake value ratio calculated to blood pool uptake; sWAT, subcutaneous white adipose tissue; vWAT, visceral white adipose tissue.

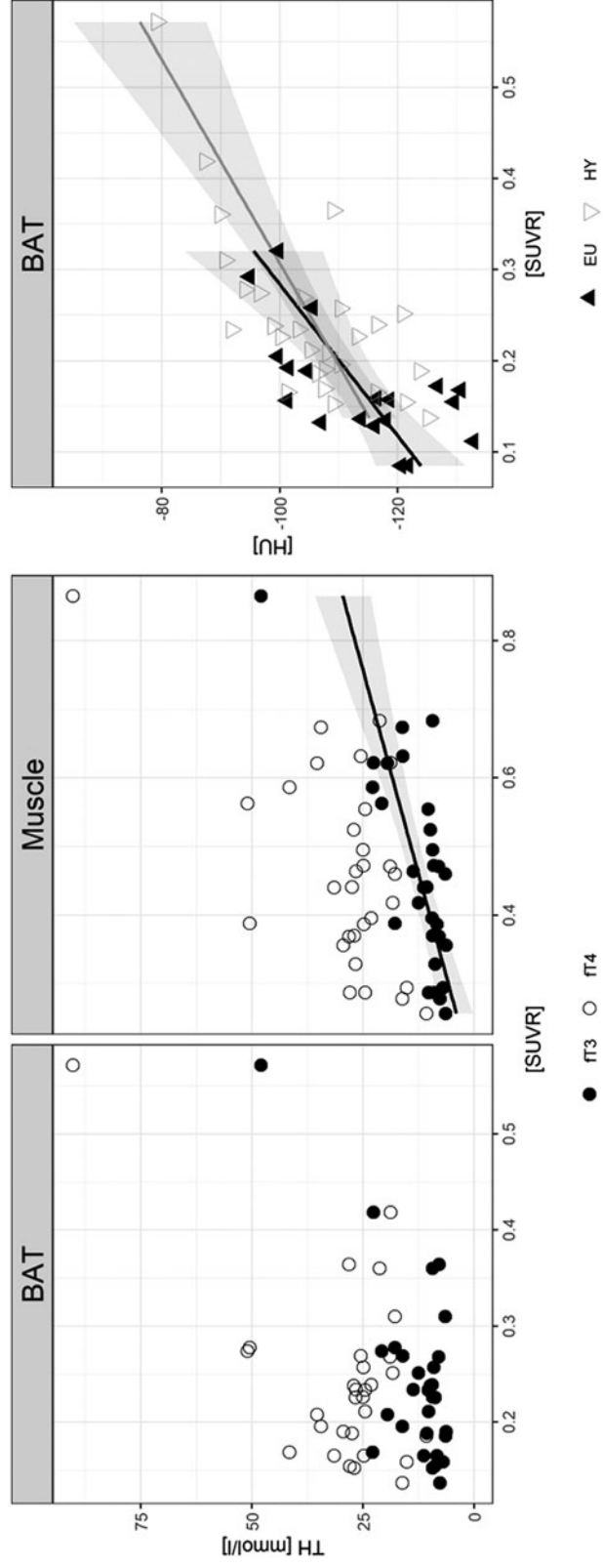


**FIG. 1.** Left: Correlation of fT3 and fT4 with BAT and muscle activation. Right: Correlation between BAT density and BAT activity in euthyroid ( $\rho = 0.62$ ;  $p = 0.005$ ) and hyperthyroid state ( $\rho = 0.564$ ;  $p < 0.001$ ). BAT, brown adipose tissue; fT3, free triiodothyronine; fT4, free thyroxine.

### Relationship between thyroid status and serum levels of adipokines and hepatokines

In grouped analyses, serum levels of fetuin A, fetuin B, RBP4, and AFABP were significantly increased in the hyperthyroid as compared with the euthyroid state. We observed no significant differences in the serum levels of FGF-21, pro-ENK, pro-NT, and NRG4 between the euthyroid and hyperthyroid state (Table 1).

Kendall-Tau correlation revealed that in the hyperthyroid state only AFABP correlated with fT3 and fT4 serum levels ( $\tau_b=0.278$ ;  $p=0.031$  and  $\tau_b=0.269$ ;  $p=0.037$ , respectively). Moreover, AFABP serum levels were positively associated with  $A_{SAT}$  ( $\tau_b=0.483$ ;  $p<0.001$ ) and negatively associated with  $A_{MTO}$  ( $\tau_b=-0.279$ ;  $p=0.034$ ). Fetuin B was positively associated with fT4 ( $\tau_b=-0.404$ ;  $p<0.05$ ; Supplementary Table S1). However, when ratios of TH serum levels in the hyper- and the euthyroid state were correlated with the respective adipokine levels, only ratio of AFABP correlated with the fT3 ratio (HY/EU) ( $\tau_b=0.359$ ;  $p=0.037$ ; Supplementary Table S3).

In the hyperthyroid state, fT3 levels and AVAT were significantly and independently associated with serum AFABP levels in the multiple regression model ( $\beta=0.419$ ;  $p=0.019$  and  $\beta=0.382$ ;  $p=0.032$ ; respectively) (Supplementary Table S4).

### Discussion

The aim of this study was to investigate the influence of TH on the areas and metabolic activity of white adipose depots and BAT in humans. Study subjects underwent 2- $^{18}\text{F}$ ]FDG-PET/CT imaging as well as detailed metabolic and anthropometric phenotyping in the hyperthyroid and euthyroid state.

In the hyperthyroid state, the total fat area, specifically areas of visceral adipose tissue, were significantly lower than in the euthyroid state. The 2- $^{18}\text{F}$ ]FDG uptake as a surrogate for glucose uptake in the supraclavicular BAT region and vWAT was significantly higher in the hyperthyroid state than in the euthyroid state. Further, we observed that the total fat area in hyperthyroidism correlated negatively with 2- $^{18}\text{F}$ ]FDG uptake in BAT, sWAT and vWAT (Supplementary Table S1). This effect was not observed when hypothyroid patients reached the euthyroid state. Although 2- $^{18}\text{F}$ ]FDG uptake in the supraclavicular BAT region was significantly higher in the hyperthyroid than in the euthyroid state, this did not correlate with fT3 or fT4 levels. Interestingly, TSH levels in the euthyroid state positively correlated with 2- $^{18}\text{F}$ ]FDG uptake in sWAT. It has been previously demonstrated that in addition to TH also TSH via the TSH receptor contributes to adipogenesis and metabolic activity of adipocytes (35–37). Altogether, these findings are most likely mediated by lipolytic effects of TH (38) and modulation of the adrenergic sensitivity of brown and white adipocytes by direct effects on postreceptor signaling (39). Accordingly, in a previous study by Lahesmaa *et al.*, an increased lipid oxidation was detected by indirect calorimetry in a cohort of hyperthyroid subjects, which suggested the increased utilization of fatty acids for BAT activation (40).

Lahesmaa *et al.* observed increased glucose uptake in skeletal muscle correlated with TH levels (40). Similarly, the total area of skeletal muscle was significantly lower in the

hyperthyroid state than in the euthyroid state in our cohort. Further, the 2- $^{18}\text{F}$ ]FDG uptake was 1.6-fold higher for the skeletal muscle of patients in the hyperthyroid state as compared with the euthyroid state. In the hyperthyroid state, we found a nominal significant association of fT4 with total skeletal muscle area. Further, the 2- $^{18}\text{F}$ ]FDG uptake of the skeletal muscle correlated negatively and significantly with fT3 levels in the hyperthyroid but not in the euthyroid state (Supplementary Tables S1 and S2). Accordingly, the higher skeletal muscle glucose uptake was likely the leading cause for changes in 2- $^{18}\text{F}$ ]FDG biodistribution, which required a semiquantitative PET analysis method. This suggests that high TH levels increase the metabolic rate through effects on the skeletal muscle rather than on BAT. These findings are in accordance with a recent study by Johann *et al.*, which showed that in mice with systemic hyperthyroidism the skeletal muscle is the primary source of peripheral hyperthermia rather than BAT (41).

The diverse effects of TH levels on adipose tissue activity, volume, dysfunction, and inflammation may be partially mediated by the action of adipokines and/or hepatokines. Consistent with previous studies, we observed increased circulating levels of AFABP, fetuin A and B in the hyperthyroid state (42–44). Fetuin-A and fetuin-B are known as hepatic markers linking fatty liver disease with glucose homeostasis and cardiometabolic risk (45,46). Plasma fetuin-A levels are known to be reduced in subjects with hypothyroidism and restored in euthyroidism (47). Moreover, fetuin-A levels are elevated in subclinical hyperthyroidism and subsequently normalized in the euthyroid status (48). Consistent with these results, fetuin A levels were significantly increased in our study cohort in the hyperthyroid state. In addition, we observed that AFABP levels in the hyperthyroid state correlated positively with fT3 and fT4 levels. Moreover, the fT3 level remained a positive independent variable associated with circulating AFABP4 levels, in addition to  $A_{VAT}$  which suggests a direct TH effect.

In summary, our study adds new perspectives on the nature of the thermogenic effects of TH in humans. We detected TH-dependent changes on glucose uptake of WAT and BAT and further observed that the hyperthyroid state particularly stimulates the activity of skeletal muscle rather than of BAT.

### Acknowledgments

The authors thank all those who participated in the studies. They would like to acknowledge excellent administrative assistance by Franziska Zientek.

### Author Disclosure Statement

No competing financial interests exist.

### Funding Information

This work was supported by grants from the German Research Foundation (Karen Geva Steinhoff 4258/3-1 to Kerstin Krause, SFB 1052 C1 to Anke Tönjes and Michael Stumvoll, DFG Priority Program SPP1629 TO 718/2-1 to Kerstin Krause, Swen Hesse, Anke Tönjes; and KR 4258/1-1 to Kerstin Krause), and from the German Diabetes Stiftung (Kerstin Krause). IFB Adiposity Diseases is supported by the Federal Ministry of Education and Research (BMBF), Germany, FKZ: 01EO1501 (AD2-7123).

## Supplementary Material

Supplementary Figure S1  
 Supplementary Table S1  
 Supplementary Table S2  
 Supplementary Table S3  
 Supplementary Table S4

## References

- Iwen KA, Schröder E, Brabant G 2013 Thyroid hormones and the metabolic syndrome. *Eur Thyroid J* **2**:83–92.
- Silva JE 2001 The multiple contributions of thyroid hormone to heat production. *J Clin Invest* **108**:35–37.
- Krause K 2020 Novel aspects of white adipose tissue browning by thyroid hormones. *Exp Clin Endocrinol Diabetes* **128**:446–449.
- Weiner J, Hankir M, Heiker JT, Fenske W, Krause K 2017 Thyroid hormones and browning of adipose tissue. *Mol Cell Endocrinol* **458**:156–159.
- Cannon B, Nedergaard J 2004 Brown adipose tissue: function and physiological significance. *Physiol Rev* **84**:277–359.
- Nedergaard J, Cannon B 2010 The changed metabolic world with human brown adipose tissue: therapeutic visions. *Cell Metab* **11**:268–272.
- Villarroya F, Cereijo R, Villarroya J, Giralt M 2017 Brown adipose tissue as a secretory organ. *Nat Rev Endocrinol* **13**:26–35.
- Christian M 2015 Transcriptional fingerprinting of “browning” white fat identifies NRG4 as a novel adipokine. *Adipocyte* **4**:50–54.
- Fisher fM, Kleiner S, Douris N, Fox EC, Mepani RJ, Verduguer F, Wu J, Kharitonov A, Flier JS, Maratos-Flier E, Spiegelman BM 2012 FGF21 regulates PGC-1 $\alpha$  and browning of white adipose tissues in adaptive thermogenesis. *Genes Dev* **26**:271–281.
- Aydogan BI, Sahin M 2013 Adipocytokines in thyroid dysfunction. *ISRN Inflamm*. DOI:10.1155/2013/646271.
- Kokkinos S, Papazoglou D, Zisimopoulos A, Papanas N, Tiaka E, Antonoglou C, Maltezos E 2016 Retinol binding protein-4 and adiponectin levels in thyroid overt and subclinical dysfunction. *Exp Clin Endocrinol Diabetes* **124**:87–92.
- Farooqi IS, O’Rahilly S 2014 20 years of leptin: human disorders of leptin action. *J Endocrinol* **223**:T63–T70.
- Wang G, Liu J, Yang N, Hu Y, Zhang H, Miao L, Yao Z, Xu Y 2016 Levothyroxine treatment restored the decreased circulating fibroblast growth factor 21 levels in patients with hypothyroidism. *Eur J Intern Med* **31**:94–98.
- Stefan N, Häring H-U 2013 Circulating fetuin-A and free fatty acids interact to predict insulin resistance in humans. *Nat Med* **19**:394–395.
- Cohade C, Osman M, Pannu HK, Wahl RL 2003 Uptake in supraclavicular area fat (“USA-Fat”): description on 18F-FDG PET/CT. *J Nucl Med* **44**:170–176.
- Brendle C, Werner MK, Schmadl M, La Fougère C, Nikolaou K, Stefan N, Pfannenbergl C 2018 Correlation of brown adipose tissue with other body fat compartments and patient characteristics: a retrospective analysis in a large patient cohort using PET/CT. *Acad Radiol* **25**:102–110.
- Lapa C, Maya Y, Wagner M, Arias-Loza P, Werner RA, Herrmann K, Higuchi T 2015 Activation of brown adipose tissue in hypothyroidism. *Ann Med* **47**:538–545.
- Nishii R, Nagamachi S, Mizutani Y, Terada T, Kiyohara S, Wakamatsu H, Fujita S, Higashi T, Yoshinaga K, Saga T, Hirai T 2018 Do TSH, FT3, and FT4 impact BAT visualization of clinical FDG-PET/CT Images? *Contrast Media Mol Imaging* **2018**:4898365.
- Cypess AM, Lehman S, Williams G, Tal I, Rodman D, Goldfine AB, Kuo FC, Palmer EL, Tseng Y-H, Doria A, Kolodny GM, Kahn CR 2009 Identification and importance of brown adipose tissue in adult humans. *N Engl J Med* **360**:1509–1517.
- Cronin CG, Prakash P, Daniels GH, Boland GW, Kalra MK, Halpern EF, Palmer EL, Blake MA 2012 Brown fat at PET/CT: correlation with patient characteristics. *Radiology* **263**:836–842.
- Zhang Q, Miao Q, Ye H, Zhang Z, Zuo C, Hua F, Guan Y, Li Y 2014 The effects of thyroid hormones on brown adipose tissue in humans: a PET-CT study. *Diabetes Metab Res Rev* **30**:513–520.
- Santhanam P, Ahima RS, Mammen JS, Giovannella L, Treglia G 2018 Brown adipose tissue (BAT) detection by 18F-FDG PET and thyroid hormone level(s)-a systematic review. *Endocrine* **62**:496–500.
- Gavrila A, Hasselgren P-O, Glasgow A, Doyle AN, Lee AJ, Fox P, Gautam S, Hennessey JV, Kolodny GM, Cypess AM 2017 Variable cold-induced brown adipose tissue response to thyroid hormone status. *Thyroid* **27**:1–10.
- Singhal V, Maffazioli GD, Ackerman KE, Lee H, Elia EF, Woolley R, Kolodny G, Cypess AM, Misra M 2016 Effect of chronic athletic activity on brown fat in young women. *PLoS One* **11**:e0156353.
- Bredella MA, Fazeli PK, Freedman LM, Calder G, Lee H, Rosen CJ, Klibanski A 2012 Young women with cold-activated brown adipose tissue have higher bone mineral density and lower Pref-1 than women without brown adipose tissue: a study in women with anorexia nervosa, women recovered from anorexia nervosa, and normal-weight women. *J Clin Endocrinol Metab* **97**:E584–E590.
- Heinen CA, Zhang Z, Klieverik LP, Wit TC de, Poel E, Yaqub M, Boelen A, Kalsbeek A, Bisschop PH, van Trotsenburg, A. S. Paul, Verberne HJ, Booij J, Fliers E 2018 Effects of intravenous thyrotropin-releasing hormone on 18F-fluorodeoxyglucose uptake in human brown adipose tissue: a randomized controlled trial. *Eur J Endocrinol* **179**:31–38.
- Chen KY, Cypess AM, Laughlin MR, Haft CR, Hu HH, Bredella MA, Enerbäck S, Kinahan PE, van Lichtenbelt WM, Lin FI, Sunderland JJ, Virtanen KA, Wahl RL 2016 Brown Adipose Reporting Criteria in Imaging Studies (BARCIST 1.0): recommendations for standardized FDG-PET/CT experiments in humans. *Cell Metab* **24**:210–222.
- Ernst A, Hellmich S, Bergmann A 2006 Proneurotensin 1–117, a stable neurotensin precursor fragment identified in human circulation. *Peptides* **27**:1787–1793.
- Boellaard R, Delgado-Bolton R, Oyen WJG, Giammarile F, Tatsch K, Eschner W, Verzijlbergen FJ, Barrington SF, Pike LC, Weber WA, Stroobants S, Delbeke D, Donohoe KJ, Holbrook S, Graham MM, Testanera G, Hoekstra OS, Zijlstra J, Visser E, Hoekstra CJ, Pruim J, Willemsen A, Arends B, Kotzerke J, Bockisch A, Beyer T, Chiti A, Krause BJ; European Association of Nuclear Medicine (EANM) 2015 FDG PET/CT: EANM procedure guidelines



- for tumour imaging: version 2.0. *Eur J Nucl Med Mol Imaging* **42**:328–354.
30. Martinez-Tellez B, Nahon KJ, Sanchez-Delgado G, Abreu-Vieira G, Llamas-Elvira JM, van Velden, Floris H P, Pereira Arias-Bouda LM, Rensen PCN, Boon MR, Ruiz JR 2018 The impact of using BARCIST 1.0 criteria on quantification of BAT volume and activity in three independent cohorts of adults. *Sci Rep* **8**:8567.
  31. Wu C, Cheng W, Sun Y, Dang Y, Gong F, Zhu H, Li N, Li F, Zhu Z 2014 Activating brown adipose tissue for weight loss and lowering of blood glucose levels: a microPET study using obese and diabetic model mice. *PLoS One* **9**: e113742.
  32. Linder N, Schaudinn A, Langenhan K, Krenzien F, Hau H-M, Benzing C, Atanasov G, Schmelzle M, Kahn T, Busse H, Bartels M, Neumann U, Wiltberger G 2019 Power of computed-tomography-defined sarcopenia for prediction of morbidity after pancreaticoduodenectomy. *BMC Med Imaging* **19**:32.
  33. Martin L, Birdsell L, Macdonald N, Reiman T, Clandinin MT, McCargar LJ, Murphy R, Ghosh S, Sawyer MB, Baracos VE 2013 Cancer cachexia in the age of obesity: skeletal muscle depletion is a powerful prognostic factor, independent of body mass index. *J Clin Oncol* **31**:1539–1547.
  34. Mullur R, Liu Y-Y, Brent GA 2014 Thyroid hormone regulation of metabolism. *Physiol Rev* **94**:355–382.
  35. Draman MS, Stechman M, Scott-Coombes D, Dayan CM, Rees DA, Ludgate M, Zhang L 2017 The role of thyrotropin receptor activation in adipogenesis and modulation of fat phenotype. *Front Endocrinol (Lausanne)* **8**:83.
  36. Elgadi A, Zemack H, Marcus C, Norgren S 2010 Tissue-specific knockout of TSHr in white adipose tissue increases adipocyte size and decreases TSH-induced lipolysis. *Biochem Biophys Res Commun* **393**:526–530.
  37. Haraguchi K, Shimura H, Lin L, Endo T, Onaya T 1996 Differentiation of rat preadipocytes is accompanied by expression of thyrotropin receptors. *Endocrinology* **137**: 3200–3205.
  38. Oppenheimer JH, Schwartz HL, Lane JT, Thompson MP 1991 Functional relationship of thyroid hormone-induced lipogenesis, lipolysis, and thermogenesis in the rat. *J Clin Invest* **87**:125–132.
  39. Rubio A, Raasmaja A, Silva JE 1995 Thyroid hormone and norepinephrine signaling in brown adipose tissue. II: differential effects of thyroid hormone on beta 3-adrenergic receptors in brown and white adipose tissue. *Endocrinology* **136**:3277–3284.
  40. Lahesmaa M, Orava J, Schalin-Jääntti C, Soinio M, Hanukainen JC, Noponen T, Kirjavainen A, Iida H, Kudomi N, Enerbäck S, Virtanen KA, Nuutila P 2014 Hyperthyroidism increases brown fat metabolism in humans. *J Clin Endocrinol Metab* **99**:E28–E35.
  41. Johann K, Cremer AL, Fischer AW, Heine M, Pensado ER, Resch J, Nock S, Virtue S, Harder L, Oelkrug R, Astiz M, Brabant G, Warner A, Vidal-Puig A, Oster H, Boelen A, López M, Heeren J, Dalley JW, Backes H, Mittag J 2019 Thyroid-hormone-induced browning of white adipose tissue does not contribute to thermogenesis and glucose consumption. *Cell Rep* **27**:3385–3400.e3.
  42. Tseng F-Y, Chen P-L, Chen Y-T, Chi Y-C, Shih S-R, Wang C-Y, Chen C-L, Yang W-S 2015 Association between serum levels of adipocyte fatty acid-binding protein and free thyroxine. *Medicine (Baltimore)* **94**:e1798.
  43. Pamuk BO, Yilmaz H, Topcuoglu T, Bilgir O, Çalan O, Pamuk G, Ertugrul DT 2013 Fetuin-A levels in hyperthyroidism. *Clinics (Sao Paulo)* **68**:379–383.
  44. Tseng F-Y, Chen Y-T, Chi Y-C, Chen P-L, Yang W-S 2018 Serum levels of fetuin-A are negatively associated with log transformation levels of thyroid-stimulating hormone in patients with hyperthyroidism or euthyroidism: an observational study at a medical center in Taiwan. *Medicine (Baltimore)* **97**:e13254.
  45. Peter A, Kovarova M, Staiger H, Machann J, Schick F, Königsrainer A, Königsrainer I, Schleicher E, Fritsche A, Häring H-U, Stefan N 2018 The hepatokines fetuin-A and fetuin-B are upregulated in the state of hepatic steatosis and may differently impact on glucose homeostasis in humans. *Am J Physiol Endocrinol Metab* **314**:E266–E273.
  46. Meex RC, Hoy AJ, Morris A, Brown RD, Lo JCY, Burke M, Goode RJA, Kingwell BA, Kraakman MJ, Febbraio MA, Greve JW, Rensen SS, Molloy MP, Lancaster GI, Bruce CR, Watt MJ 2015 Fetuin B is a secreted hepatocyte factor linking steatosis to impaired glucose metabolism. *Cell Metab* **22**:1078–1089.
  47. Bakiner O, Bozkirli E, Ertugrul D, Sezgin N, Ertorer E 2014 Plasma fetuin-A levels are reduced in patients with hypothyroidism. *Eur J Endocrinol* **170**:411–418.
  48. Bilgir O, Bilgir F, Topcuoglu T, Calan M, Calan O 2014 Comparison of high-sensitivity C-reactive protein and fetuin-A levels before and after treatment for subjects with subclinical hyperthyroidism. *Endocrine* **45**:244–248.

Address correspondence to:

Anke Tönjes, MD  
 Medical Department III–Endocrinology,  
 Nephrology, Rheumatology  
 University of Leipzig Medical Center  
 Liebigstraße 20  
 Leipzig D-04103  
 Germany

E-mail: anke.toenjes@medizin.uni-leipzig.de

Swen Hesse, MD  
 Department of Nuclear Medicine  
 University of Leipzig Medical Center  
 Liebigstraße 18  
 Leipzig D-04103  
 Germany

E-mail: swen.hesse@medizin.uni-leipzig.de